

Many-body radiative decay in strongly interacting Rydberg ensembles

Chris Nill,¹ Kay Brandner,² Beatriz Olmos,^{1,2} Federico Carollo,¹ and Igor Lesanovsky^{1,2}

¹*Institut für Theoretische Physik, Universität Tübingen,
Auf der Morgenstelle 14, 72076 Tübingen, Germany*

²*School of Physics and Astronomy and Centre for the Mathematics
and Theoretical Physics of Quantum Non-Equilibrium Systems,
The University of Nottingham, Nottingham, NG7 2RD, United Kingdom*

When atoms are excited to high-lying Rydberg states they interact strongly with dipolar forces. The resulting state-dependent level shifts allow to study many-body systems displaying intriguing nonequilibrium phenomena, such as constrained spin systems, and are at the heart of numerous technological applications, e.g., in quantum simulation and computation platforms. Here, we show that these interactions have also a significant impact on dissipative effects caused by the inevitable coupling of Rydberg atoms to the surrounding electromagnetic field. We demonstrate that their presence modifies the frequency of the photons emitted from the Rydberg atoms, making it dependent on the local neighborhood of the emitting atom. Interactions among Rydberg atoms thus turn spontaneous emission into a many-body process which manifests, in a thermodynamically consistent Markovian setting, in the emergence of collective jump operators in the quantum master equation governing the dynamics. We discuss how this collective dissipation — stemming from a mechanism different from the much studied super- and sub-radiance — accelerates decoherence and affects dissipative phase transitions in Rydberg ensembles.

Introduction — Rydberg gases allow to explore the interplay between strong interactions, external driving imposed by external fields and dissipation. This has led to a whole host of theoretical and experimental works, investigating, for example, dissipative phase transitions, the dynamics of epidemic spreading and critical phenomena [1–6], as well as the dissipative preparation of correlated quantum states [7–10]. Dissipation typically manifests through two processes, which are decoherence (of quantum superposition) and radiative decay [11–14]. Decoherence leads to a gradual decay of quantum superposition that is formed between the high-lying Rydberg state and the atomic ground state from which the Rydberg state is excited. This process can be controlled by the phase-coherence of the excitation laser and by the temperature of the Rydberg gas. It is also influenced by strong interactions among Rydberg atoms [14–17], which can be exploited for designing single photon absorbers and emitters [18–22]. Radiative decay, on the other hand, is an ubiquitous process which is caused by the coupling of the atomic dipole to the electromagnetic field. This results in the spontaneous emission of a photon from a Rydberg excited atom and a concomitant quantum jump from the Rydberg state to a low-lying electronic state, e.g., the ground state.

When considering ensembles of atoms, their coupling to the radiation field [23, 24] can lead to collective behavior as pointed out by Dicke in his seminal work [25]. This emerges when the typical distance between the atoms becomes comparable to the wavelength of the emitted radiation. In this case it is no longer possible to trace an emitted photon back to a specific atom. This loss of ‘which way’-information results in quantum interference that ultimately promotes this dissipation from a single-atom to a many-atom process. A striking consequence of this is

the appearance of sub-radiant collective states whose lifetime may exceed that of single atoms by orders of magnitude [26–33]. In typical experiments, Rydberg atoms are separated by several micrometers. This is significantly larger than the wavelength for transitions to low-lying states, which is on the order of hundred nanometers. Radiative decay is therefore here not expected to acquire a collective character and is typically modelled as a single-atom process. Note, that super- and subradiance can nevertheless occur – and have been investigated – in Rydberg gases [34–37]. However, in these studies the considered radiative transitions take place among Rydberg states and the associated wavelengths are on the order of millimetres to centimetres [38].

In this work we demonstrate that strong interactions in Rydberg gases can nevertheless be responsible for another mechanism underlying collective dissipation. The fundamental observation is that the frequency of a photon that is spontaneously emitted from a decaying Rydberg atom depends on the state of the neighborhood of the emitting atom [cf. Fig. 1(a-b)]. We unveil this effect and analyze its consequences in a simple setting, permitting for the exact derivation of the Markovian quantum master equation of the Rydberg gas which, as we discuss, features many-body jump operators. We show that the ensuring dissipation accelerates decoherence and that it further impacts on nonequilibrium phase transitions occurring in the stationary state of driven Rydberg gases. This collective *state-dependent* decay mechanism should be observable in (precision) experiments and is important for a thermodynamically consistent and faithful modelling of noise and error sources in quantum computers and simulators based on Rydberg atoms.

Interacting Rydberg gas in an electromagnetic field — To illustrate the above-mentioned effect we focus on a

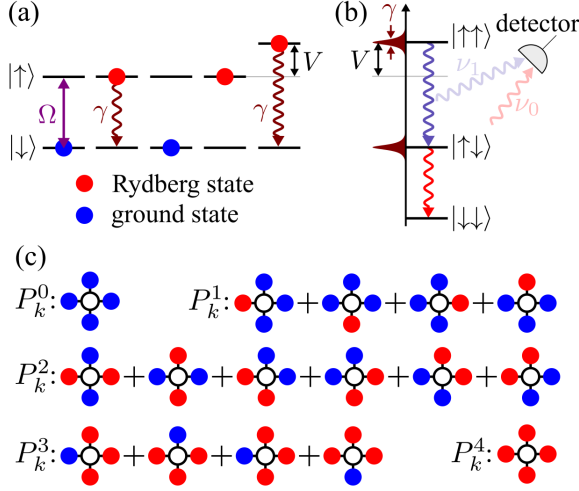


FIG. 1. **Rydberg atoms and collective dissipation.** (a) One-dimensional lattice gas of interacting atoms resonantly driven by a laser with Rabi frequency Ω . Neighboring atoms interact with interaction strength V when simultaneously excited to their Rydberg state $|\uparrow\rangle$. Rydberg states decay under the emission of a photon to the ground state, $|\downarrow\rangle$, at rate γ . (b) Decay in a system of two atoms. When the interaction strength V is larger than the natural linewidth γ it is possible to discern whether a decaying Rydberg atom had an excited neighboring atom or not. This information can be inferred from the frequency of the emitted photon; ν_1 : excited neighboring atom, ν_0 : neighboring atom in the ground state. (c) Graphical representation of projectors P_k^ξ which project on the subspace where the neighborhood of a reference atom (empty circle) contains ξ excited atoms (in two dimensions). Due to the strong nearest-neighbor interaction an emitted photon carries information on the subspace from which the emission took place, leading to collective jump operators.

simple model of a Rydberg gas. The atoms are placed on the sites of a d -dimensional hypercubic lattice, labeled by the position vectors \mathbf{r}_k . Each atom is effectively described as a two-level (spin) system [see sketch in Fig. 1(a)], with ground state $|\downarrow\rangle$ and Rydberg state $|\uparrow\rangle$ separated by an energy difference ω_a . We also assume for simplicity that the atoms only interact with their nearest neighbors with coupling strength V [see Fig. 1(a)]. This is accounted for by the Hamiltonian

$$H_{\text{atom}} = \omega_a \sum_k n_k + \frac{V}{2} \sum_{|k-m|=1} n_k n_m, \quad (1)$$

where $n_k = |\uparrow_k\rangle\langle\uparrow_k|$ is the projector on the Rydberg state of the atom located at position \mathbf{r}_k .

The atoms are immersed in an electromagnetic radiation field, described by the Hamiltonian

$$H_{\text{rad}} = \sum_{\mathbf{q},s} \omega_q a_{\mathbf{q}s}^\dagger a_{\mathbf{q}s}. \quad (2)$$

Here, $a_{\mathbf{q}s}$ and $a_{\mathbf{q}s}^\dagger$ are the annihilation and creation operators of a photon mode with momentum \mathbf{q} , polarization

s , and energy $\omega_q = c|\mathbf{q}|$ (c is the speed of light). The dipole coupling between the atoms and the electromagnetic field modes is determined by the interaction Hamiltonian

$$H_{\text{int}} = \sum_{k,\mathbf{q},s} (g_{\mathbf{q}s} a_{\mathbf{q}s}^\dagger e^{i\mathbf{q}\cdot\mathbf{r}_k} + \text{h.c.}) (\sigma_k^+ + \sigma_k^-). \quad (3)$$

Here, $\sigma_k^+ = (\sigma_k^-)^\dagger = |\uparrow_k\rangle\langle\downarrow_k|$ is the atomic raising operator for the atom located at \mathbf{r}_k . The coupling constant $g_{\mathbf{q}s} = \sqrt{\frac{\omega_q}{2\epsilon_0 V}} (\mathbf{d} \cdot \boldsymbol{\epsilon}_s)$ depends on the atomic transition dipole moment \mathbf{d} , the unit polarization vector $\boldsymbol{\epsilon}_s$, the vacuum permittivity ϵ_0 and the quantization volume V .

Our aim is to integrate out the electromagnetic field modes in order to obtain a quantum master equation that describes the open quantum dynamics of the atomic ensemble. We follow a procedure analogous to the usual one developed for the description of non-interacting atoms immersed in the radiation field (see e.g. Refs. [23, 24]). First, we rotate into the interaction picture with respect to the atom and radiation degrees of freedom via the unitary transformation $U = \exp[it(H_{\text{atom}} + H_{\text{rad}})]$. Due to the Rydberg interactions, atomic operators acquire an operator-valued phase which depends on the neighborhood of the considered atom, e.g.,

$$U \sigma_k^+ U^\dagger = \sigma_k^+ \exp(i\omega_a t) \exp\left(iVt \sum_{\xi=0}^{2d} \xi P_k^\xi\right). \quad (4)$$

Here, $\xi \in \{0, 1, \dots, 2d\}$ and P_k^ξ is the projector on the subspace containing exactly ξ excited atoms in the neighborhood of atom k [see Fig. 1(c)]. Similar structures emerge, for example, in the so-called PXP model or the quantum hard-squares model, which describe strongly interacting Rydberg gases [39, 40].

As derived in the Supplementary Material [41], after the Born-Markov and rotating-wave approximations, the quantum master equation reads (in the original lab frame):

$$\dot{\rho} = -i[H_{\text{atom}}, \rho] + \gamma \sum_k \left[\sum_{\xi=0}^{2d} P_k^\xi \sigma_k^- \rho \sigma_k^+ P_k^\xi - \frac{1}{2} \{n_k, \rho\} \right], \quad (5)$$

where $\gamma = (|\mathbf{d}|^2 \omega_a^3) / (3\pi c^3 \epsilon_0)$ is the single atom decay rate. Note, that for the rotating-wave approximation to be valid the nearest-neighbor interaction strength V must be much larger than γ . Moreover, we have assumed that $\omega_a \gg V$, which allows us to neglect corrections to the spontaneous emission rate originating from the interaction shift of the atomic levels in the presence of neighboring excitations, which are of order ω_a/V . Finally, note that we consider the separation between neighboring atoms to be much larger than the transition wavelength $\lambda = 2\pi c/\omega_a$. This allows us to neglect the effect

of coherent dipole-dipole interactions and collective dissipation (i.e. super- and subradiance) induced by the radiation field.

From the form of the master equation (5) it becomes evident that an atom at position \mathbf{r}_k has $2d + 1$ different decay channels, where d is the dimension of the hypercubic lattice on which the atoms are positioned. Each of these channels, which is represented by the collective many-body jump operator $L_k^c = \sqrt{\gamma} P_k^\xi \sigma_k^-$ corresponds to a different number of excited atoms ξ in the atom's neighborhood, and can be associated to a different frequency of the emitted photons, $\nu_\xi = \omega_a + \xi V$ [see Fig. 1(b)].

The many-body operators L_k^c are also consistent with thermodynamic considerations. While we treat the background radiation field as an effective zero-temperature reservoir here, which is well justified since the atomic energy scale ω_a is typically much larger than the temperatures encountered in quantum-optical experiments, it is in principle straightforward to extend our approach to thermal environments with finite inverse temperature β . One would then expect the Gibbs state $\propto \exp[-\beta(H_{\text{atom}})]$ to be a stationary state of the corresponding master equation. This condition, which is indeed met in our many-body approach, is also both sufficient and necessary for consistency with the second law of thermodynamics, at least in situations where the standard weak-coupling, Born-Markov and rotating-wave approximations are applicable [45, 46]. On the other hand, a simpler model in which each atom would feature a single decay channel, represented by a jump operator $L_k^s = \sqrt{\gamma} \sigma_k^-$ that does not account for interactions between atoms, would lead to a non-thermal stationary state at finite temperatures and thus, in general, to violations of the second law, see also Ref. [47].

Decoherence dynamics — In order to analyze the impact of collective jump operators versus the conventionally employed single-atom decay, we consider an atomic ensemble that is initially prepared in the state $|\Psi_0\rangle = (1/2)^{N/2} \prod_k [|\downarrow\rangle_k + |\uparrow\rangle_k]$. We study the evolution of the average single-atom (Rydberg state - ground state) coherence, which can be measured experimentally [48], and which we decompose as

$$X(t) = \frac{1}{N} \sum_k \langle \sigma_k^- \rangle(t) = \frac{1}{N} \sum_{k,\xi} \langle P_k^\xi \sigma_k^- \rangle(t) = \sum_\xi X_\xi(t). \quad (6)$$

Using the adjoint master equation, the evolution equation of the expectation values X_ξ is readily obtained [41]. For the collective dissipation, described by Eq. (5), we obtain

$$\dot{X}_\xi^c = -\left(i\omega_a + \frac{\gamma}{2}\right) X_\xi^c - \xi(\gamma + iV) X_\xi^c,$$

while the conventionally employed single-atom decay

yields [41]

$$\dot{X}_\xi^s = -\left(i\omega_a + \frac{\gamma}{2}\right) X_\xi^s - \xi(\gamma + iV) X_\xi^s + \gamma(\xi + 1) X_{\xi+1}^s,$$

where we use the convention $X_{2d+1}^s = 0$. These equations can be straight-forwardly integrated with the initial condition $X_\xi^{s/c}(0) = (1/N) \sum_k \langle \Psi_0 | P_k^\xi \sigma_k^- | \Psi_0 \rangle = 2^{-2d-1} \binom{2d}{\xi}$. In the subsequent analysis, we focus on the short-time behavior, which already displays a qualitative difference between collective dissipation and single-body decay:

$$|X^s(t)| \approx \frac{1}{2} - \frac{1}{4}\gamma t + \frac{\gamma^2 - 2dV^2}{16} t^2, \\ |X^c(t)| \approx \frac{1}{2} - \frac{2d+1}{4}\gamma t + \frac{[(2d+1)^2 + 2d]\gamma^2 - 2dV^2}{16} t^2.$$

For single-atom decay the initial drop of the coherence from its initial value $1/2$ is independent of the system geometry. The first collective contribution to decoherence emerges from the interaction of an atom with its neighbors, which involves the interaction strength V and the coordination number $2d$ and is thus not of dissipative nature. In contrast, for the case of collective decay, already the leading term is dependent on the coordination number. This shows that collective dissipation notably accelerates the decoherence process as compared to the single-atom case.

This effect should be even more dramatic in a continuous gas. Here, the initial rate of decoherence is proportional to the number of atoms, N_{int} , with which a given reference atom interacts strongly enough so that the concomitant energy shift exceeds the single atom decay rate γ . For a homogeneous atomic gas with density ρ_0 and Rydberg states that are interacting with a van-der-Waals potential [38], $V_{\text{vdW}}(r) = C_6/r^6$, this number of atoms scales as $N_{\text{int}} \sim \rho_0 (|C_6|/\gamma)^{d/6}$ and thus the collective decoherence rate should scale as $\gamma_c \sim \gamma \rho_0 (C_6/\gamma)^{d/6}$.

Stationary state of a laser-driven Rydberg gas — The stationary state of the dynamics considered so far is the one devoid of any Rydberg excitation, since the system is only coupled with an effectively zero-temperature reservoir. In the following we are interested in exploring the stationary state that emerges when (collective) radiative decay competes with external laser driving. To include the excitation laser (with Rabi frequency Ω and detuning Δ) we consider master equation (5) with the modified atomic Hamiltonian

$$H_{\text{atom}} \rightarrow H_{\text{atom}} + \sum_k [\Omega \sigma_k^x + (\Delta - \omega_a) n_k]. \quad (7)$$

This is actually an *ad-hoc* construction, given that the master equation has to be derived using the modified Hamiltonian. However, this approach is currently the standard one for incorporating coherent laser excitation, interaction and dissipation in interacting Rydberg gases [4, 11, 14, 49]. Our expectation at this point is that its analysis will reveal which quantitative and qualitative

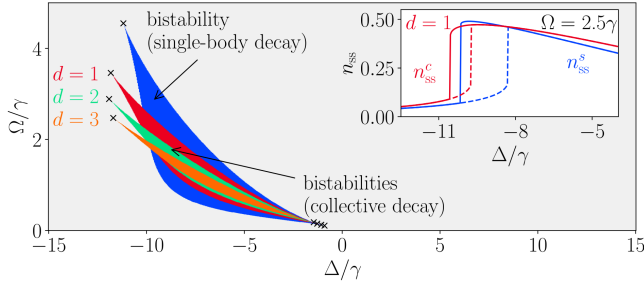


FIG. 2. **Bistability region in the mean field phase diagram in the presence of single-atom and collective decay.** In the grey region the stationary state of the mean field equations is unique. In the colored region, whose shape depends on the dimension d , two stationary solutions exist. The cusps culminate in critical points, which are marked by crosses. The inset shows a cut of the stationary state density through the bistability region, taken at $\Omega = 2.5\gamma$. The red (blue) curves show the stationary Rydberg excitation density n_{ss}^c (n_{ss}^s) in the case of collective (single-atom) decay. Solid and dashed lines mark the two stationary solutions. We have set $dV = 10\gamma$.

changes to the stationary state — caused by collective jump operators — one may expect.

We first perform a mean field analysis. Following the treatment of Ref. [2], this leads to the mean field equations of motion

$$\begin{aligned} \dot{n} &= \Omega s_y - \gamma n \\ \dot{s}_x &= -\Delta s_y - \frac{\gamma}{2}(4dn + 1)s_x - 2dVns_y \\ \dot{s}_y &= -\Delta s_x - \frac{\gamma}{2}(4dn + 1)s_y + 2dVns_x - \Omega(4n - 2). \end{aligned} \quad (8)$$

Here, $n = \langle n_k \rangle$, $s_x = \langle \sigma_x^k \rangle$ and $s_y = \langle \sigma_y^k \rangle$ and translation invariance is assumed throughout. A noteworthy aspect of these equations is their dependence on the dimension d . In the contribution due to interactions, the latter enters through the combination $2dV$, with $2d$ being the coordination number of the d -dimensional hypercubic lattice. Therefore, different dimensions simply lead to a rescaling of the mean field interaction. This is not the case for the collective decay which results in terms proportional to $\gamma(4dn + 1)$, which does not amount to a simple rescaling when changing dimensionality. This becomes visible in the stationary state phase diagram displayed in Fig. 2. In the main figure we show the number of stable stationary mean field solutions. While for most parameters there is merely one solution, there exists a region for which two stationary solutions emerge [2, 50]. Here the system may feature bistable (or meta-stable) behavior [2, 4], as shown in the inset. From a dynamical perspective this typically manifests in intermittency of the quantum jump statistics [1, 51, 52]. The important aspect here is that the size and shape of this region strongly depend on the dimensionality, which is not the case when single-body decay is considered where one can

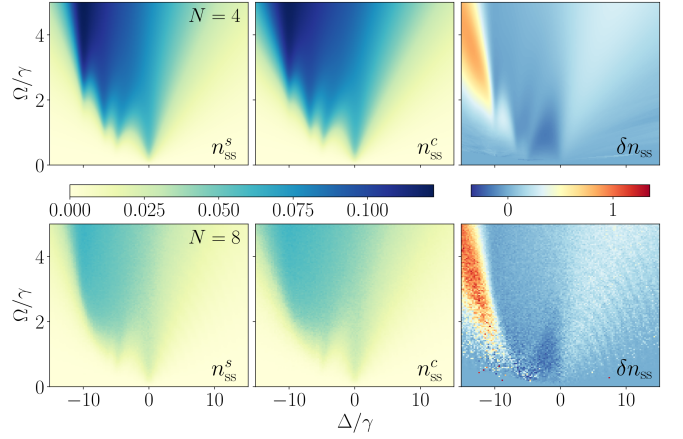


FIG. 3. **Stationary state of a $d = 1$ chain with periodic boundaries.** Shown is the stationary density of Rydberg excitations as a function of the laser detuning Δ and the Rabi frequency Ω with $V = 10\gamma$ in the presence of single-body decay (n_{ss}^s) and collective many-body decay (n_{ss}^c). In the right-most column we show the relative difference between the two densities, $\delta n_{ss} = (n_{ss}^c - n_{ss}^s)/n_{ss}^s$. Significant deviations are visible for negative detunings in the region where bistable behavior is predicted by the mean field analysis. To estimate the steady state we average over 100 linearly spaced data points in the interval $[4.75\gamma t, 5.00\gamma t]$. The oscillations visible in the region $\Delta/\gamma > 0$ are a finite time effect. The data for $N = 4$ is obtained by exact diagonalization, while the $N = 8$ data was calculated using continuous-time quantum jump Monte Carlo averaged over 300 trajectories.

simply rescale the interaction strength.

To complement the mean field analysis we numerically calculate the stationary state of a small one-dimensional chain containing either $N = 4$ or $N = 8$ atoms. Qualitatively, both single-body and collective decay yield similar results, which are displayed in Fig. 3. For negative detunings Δ — where the mean field analysis predicts bistable behavior — there is however a substantial quantitative difference. For example, the excitation density under collective dissipation can exceed the one predicted by single-atom decay by more than a factor two. This indicates that the bistable or metastable (in low dimensions) regions indeed are located in different regions of the parameter space, as the mean field result suggests.

Conclusions and future directions — In this work we have studied the radiative decay of an interacting Rydberg gas. We have considered a rather simplified scenario, in which Rydberg atoms interact with nearest-neighbor interaction V , whose value exceeds that of the emission linewidth γ . Realistic interactions have a gradually decaying tail and there will be distances in which the interaction strength between the atoms becomes comparable with the decay rate. Here it is no longer possible to perform a rotating-wave approximation and the master equation becomes explicitly time dependent. Moreover, it would be interesting to include the laser driv-

ing systematically in the derivation of the master equation for the atomic system, e.g., by using the Floquet-Lindblad approach, which makes it possible to accommodate strong periodic driving fields in a thermodynamically consistent way [53]. For the sake of simplicity, we have focused on an ad-hoc approach in this article, where the driving is incorporated only in the unitary part of the master equation, as is currently standard quantum optics.

In order to experimentally probe the impact of collective effects it would be desirable to investigate strongly interacting Rydberg lattice systems that allow to observe dissipative dynamics over many emission cycles. This should be, for example, possible in trapped Rydberg ion systems [54, 55], which provide trapping of ground and Rydberg states alike and also offer the opportunity to continuously cool external degrees of freedom that may be heated from spontaneous emission.

Acknowledgements — The research leading to these results has received funding from the “Wissenschaftler-Rückkehrprogramm GSO/CZS” of the Carl-Zeiss-Stiftung and the German Scholars Organization e.V., through the Deutsche Forschungsgemeinschaft (DFG, German Research Foundation) under Projects No. 435696605 and 449905436, as well as through the Research Unit FOR 5413/1, Grant No. 465199066. We also acknowledge support from the Baden-Württemberg Stiftung through Project No. BWST-ISF2019-23. This work was supported by the University of Nottingham and the University of Tübingen’s funding as part of the Excellence Strategy of the German Federal and State Governments, in close collaboration with the University of Nottingham. K.B. acknowledges support from the University of Nottingham through a Nottingham Research Fellowship. This work was supported by the Medical Research Council [grant number MR/S034714/1; and the Engineering and Physical Sciences Research Council [grant number EP/V031201/1]. F.C. is indebted to the Baden-Württemberg Stiftung for the financial support by the Eliteprogramme for Postdocs.

[1] N. Malossi, M. M. Valado, S. Scotto, P. Huillery, P. Pillet, D. Ciampini, E. Arimondo, and O. Morsch, *Phys. Rev. Lett.* **113**, 023006 (2014).
[2] M. Marcuzzi, E. Levi, S. Diehl, J. P. Garrahan, and I. Lesanovsky, *Phys. Rev. Lett.* **113**, 210401 (2014).
[3] A. Urvoy, F. Ripka, I. Lesanovsky, D. Booth, J. P. Schaffer, T. Pfau, and R. Löw, *Phys. Rev. Lett.* **114**, 203002 (2015).
[4] F. Letscher, O. Thomas, T. Niederprüm, M. Fleischhauer, and H. Ott, *Phys. Rev. X* **7**, 021020 (2017).
[5] R. Gutiérrez, C. Simonelli, M. Archimi, F. Castellucci, E. Arimondo, D. Ciampini, M. Marcuzzi, I. Lesanovsky, and O. Morsch, *Phys. Rev. A* **96**, 041602 (2017).
[6] S. Helmrich, A. Arias, G. Lochead, T. Wintermantel,

M. Buchhold, S. Diehl, and S. Whitlock, *Nature* **577**, 481 (2020).
[7] B. Kraus, H. P. Büchler, S. Diehl, A. Kantian, A. Micheli, and P. Zoller, *Phys. Rev. A* **78**, 042307 (2008).
[8] A. W. Carr and M. Saffman, *Phys. Rev. Lett.* **111**, 033607 (2013).
[9] M. Hönig, D. Muth, D. Petrosyan, and M. Fleischhauer, *Phys. Rev. A* **87**, 023401 (2013).
[10] D. Petrosyan, M. Hönig, and M. Fleischhauer, *Phys. Rev. A* **87**, 053414 (2013).
[11] R. Löw, H. Weimer, J. Nipper, J. B. Balewski, B. Butscher, H. P. Büchler, and T. Pfau, *J. Phys. B* **45**, 113001 (2012).
[12] M. Gärtner, S. Whitlock, D. W. Schönleber, and J. Evers, *Phys. Rev. Lett.* **113**, 233002 (2014).
[13] M. Marcuzzi, J. Schick, B. Olmos, and I. Lesanovsky, *J. Phys. A* **47**, 482001 (2014).
[14] E. Guardado-Sanchez, P. T. Brown, D. Mitra, T. Devakul, D. A. Huse, P. Schauß, and W. S. Bakr, *Phys. Rev. X* **8**, 021069 (2018).
[15] F. Letscher, O. Thomas, T. Niederprüm, H. Ott, and M. Fleischhauer, *Phys. Rev. A* **95**, 023410 (2017).
[16] A. Signoles, T. Franz, R. Ferracini Alves, M. Gärtner, S. Whitlock, G. Zürn, and M. Weidemüller, *Phys. Rev. X* **11**, 011011 (2021).
[17] P. Schultzen, T. Franz, S. Geier, A. Salzinger, A. Tebben, C. Hainaut, G. Zürn, M. Weidemüller, and M. Gärtner, *Phys. Rev. B* **105**, L020201 (2022).
[18] F. Bariani, Y. O. Dudin, T. A. B. Kennedy, and A. Kuzmich, *Phys. Rev. Lett.* **108**, 030501 (2012).
[19] Y. Dudin and A. Kuzmich, *Science* **336**, 887 (2012).
[20] J. Honer, R. Löw, H. Weimer, T. Pfau, and H. P. Büchler, *Phys. Rev. Lett.* **107**, 093601 (2011).
[21] C. Tresp, C. Zimmer, I. Mirgorodskiy, H. Gorniaczyk, A. Paris-Mandoki, and S. Hofferberth, *Phys. Rev. Lett.* **117**, 223001 (2016).
[22] N. Stiesdal, H. Busche, K. Kleinbeck, J. Kumlin, M. G. Hansen, H. P. Büchler, and S. Hofferberth, *Nat. Commun.* **12**, 4328 (2021).
[23] R. H. Lehmberg, *Phys. Rev. A* **2**, 883 (1970).
[24] D. F. V. James, *Phys. Rev. A* **47**, 1336 (1993).
[25] R. H. Dicke, *Phys. Rev.* **93**, 99 (1954).
[26] A. Asenjo-Garcia, M. Moreno-Cardoner, A. Albrecht, H. J. Kimble, and D. E. Chang, *Phys. Rev. X* **7**, 031024 (2017).
[27] J. A. Needham, I. Lesanovsky, and B. Olmos, *New J. Phys.* **21**, 073061 (2019).
[28] O. Rubies-Bigorda, V. Walther, T. L. Patti, and S. F. Yelin, *Phys. Rev. Research* **4**, 013110 (2022).
[29] Y.-X. Zhang, C. Yu, and K. Mølmer, *Phys. Rev. Research* **2**, 013173 (2020).
[30] G. Facchinetti, S. D. Jenkins, and J. Ruostekoski, *Phys. Rev. Lett.* **117**, 243601 (2016).
[31] W. Guerin, M. O. Araújo, and R. Kaiser, *Phys. Rev. Lett.* **116**, 083601 (2016).
[32] J. Rui, D. Wei, A. Rubio-Abadal, S. Hollerith, J. Zeiher, D. M. Stamper-Kurn, C. Gross, and I. Bloch, *Nature* **583**, 374 (2020).
[33] G. Ferioli, A. Glicenstein, L. Henriët, I. Ferrier-Barbut, and A. Browaeys, *Phys. Rev. X* **11**, 021031 (2021).
[34] M. Gross, P. Goy, C. Fabre, S. Haroche, and J. M. Raimond, *Phys. Rev. Lett.* **43**, 343 (1979).
[35] T. Wang, S. F. Yelin, R. Côté, E. E. Eyler, S. M. Farooqi, P. L. Gould, M. Kostrun, D. Tong, and D. Vranceanu,

- Phys. Rev. A **75**, 033802 (2007).
- [36] L. Hao, Z. Bai, J. Bai, S. Bai, Y. Jiao, G. Huang, J. Zhao, W. Li, and S. Jia, New J. Phys. **23**, 083017 (2021).
 - [37] E. Suarez, P. Wolf, P. Weiss, and S. Slama, Phys. Rev. A **105**, L041302 (2022).
 - [38] M. Saffman, T. G. Walker, and K. Mølmer, Rev. Mod. Phys. **82**, 2313 (2010).
 - [39] B. Sun and F. Robicheaux, New J. Phys. **10**, 045032 (2008).
 - [40] I. Lesanovsky, Phys. Rev. Lett. **106**, 025301 (2011).
 - [41] See the Supplemental Material, which further contains Refs. [42–44], for details.
 - [42] H.-P. Breuer and F. Petruccione, *The theory of open quantum systems* (Oxford University Press, 2002).
 - [43] A. G. Redfield, IBM J. Res. Dev. **1**, 19 (1957).
 - [44] R. M. Wilcox, J. Math. Phys. **8**, 962 (1967).
 - [45] H. Spohn, J. Math. Phys. **19**, 1227 (1978).
 - [46] K. Brandner and U. Seifert, Phys. Rev. E **93**, 062134 (2016).
 - [47] A. Levy and R. Kosloff, Europhys. Lett. **107**, 20004 (2014).
 - [48] G. Semeghini, H. Levine, A. Keesling, S. Ebadi, T. T. Wang, D. Bluvstein, R. Verresen, H. Pichler, M. Kalinowski, R. Samajdar, *et al.*, Science **374**, 1242 (2021).
 - [49] M. Morgado and S. Whitlock, AVS Quantum Science **3**, 023501 (2021).
 - [50] T. E. Lee, H. Häffner, and M. C. Cross, Phys. Rev. A **84**, 031402 (2011).
 - [51] T. E. Lee, H. Häffner, and M. C. Cross, Phys. Rev. Lett. **108**, 023602 (2012).
 - [52] C. Ates, B. Olmos, J. P. Garrahan, and I. Lesanovsky, Phys. Rev. A **85**, 043620 (2012).
 - [53] R. Kosloff, Entropy **15**, 2100 (2013).
 - [54] F. Schmidt-Kaler, T. Feldker, D. Kolbe, J. Walz, M. Müller, P. Zoller, W. Li, and I. Lesanovsky, New J. Phys. **13**, 075014 (2011).
 - [55] C. Zhang, F. Pokorny, W. Li, G. Higgins, A. Pöschl, I. Lesanovsky, and M. Hennrich, Nature **580**, 345 (2020).

SUPPLEMENTAL MATERIAL

Many-body radiative decay in strongly interacting Rydberg ensembles

Chris Nill¹, Kay Brandner², Beatriz Olmos^{1,2}, Federico Carollo¹ and Igor Lesanovsky^{1,2}

¹*Institut für Theoretische Physik, Universität Tübingen,
Auf der Morgenstelle 14, 72076 Tübingen, Germany*

²*School of Physics and Astronomy and Centre for the Mathematics and Theoretical Physics of Quantum
Non-Equilibrium Systems, The University of Nottingham, Nottingham, NG7 2RD, United Kingdom*

I. DERIVATION OF THE MASTER EQUATION WITH COLLECTIVE JUMP OPERATORS

In this section we derive equation (5) from the main paper. We start with the *Redfield equation*, where the Born-Markov approximations have already been assumed [42, 43]. We label the trace over the bath degrees of freedom with $\text{tr}_E \{ \cdot \}$ and the Hamiltonian in the interaction picture with $H''(t)$. The time evolution of the system at time t is exclusively dependent on the current state $\rho_{\text{int}}(t) =: \rho_{\text{int}}$ in the rotating frame and reads:

$$\dot{\rho}_{\text{int}} = - \int_0^t d\tau \text{tr}_E \{ [H''(t), [H''(\tau), \rho_{\text{int}} \otimes \rho_E(0)]] \}. \quad (\text{S1})$$

To obtain a Markovian master equation, the explicit dependence on the absolute time t must be eliminated. We therefore substitute $\tau = t - t'$ into (S1) and assume that the bath correlation time τ_E is sufficiently small compared to τ ($\tau_E \ll \tau$). The integrand thus decays sufficiently fast, and the upper integration limit can be considered to be infinity to a good approximation. We now obtain the Markovian quantum master equation:

$$\dot{\rho}_{\text{int}} = - \int_0^\infty d\tau \text{tr}_E \{ [H''(t), [H''(t - \tau), \rho_{\text{int}} \otimes \rho_E(0)]] \}. \quad (\text{S2})$$

It should be noted that the above equation does not resolve the dynamics on time scales of the correlation time τ_E . In this sense, the equation describes a coarse-grained time evolution. In the later calculation, we have to perform a rotating wave approximation (also called *secular approximation*) which means that we have to neglect fast oscillating terms in the order of magnitude of the correlation time τ_E by averaging. Only in this way, we end up with a Markovian master equation that is a generator of a quantum dynamical semigroup [42].

The Hamiltonian of the whole system is obtained by summing up Eq. (1), (2) and (3) from the main paper:

$$H = \underbrace{\omega_a \sum_k n_k + \frac{V}{2} \sum_{\langle km \rangle} n_k n_m}_{H_{\text{atom}}} + \underbrace{\sum_{\mathbf{q}s} \omega_q a_{\mathbf{q}s}^\dagger a_{\mathbf{q}s}}_{H_{\text{rad}}} + \underbrace{\sum_{k, \mathbf{q}, s} (g_{\mathbf{q}s} a_{\mathbf{q}s}^\dagger e^{i\mathbf{q} \cdot \mathbf{r}_k} + \text{h.c.}) (\sigma_k^+ + \sigma_k^-)}_{H_{\text{int}}}. \quad (\text{S3})$$

We transform H into the interaction picture via a unitary transformation:

$$H''(t) = U H_{\text{int}} U^\dagger \quad (\text{S4})$$

$$U = e^{it(H_{\text{atom}} + H_{\text{rad}})}. \quad (\text{S5})$$

We then use the Baker-Campbell-Hausdorff formula [44] to simplify H'' and subsequently obtain:

$$H''(t) = \sum_{k, \mathbf{q}, s} (g_{\mathbf{q}s} a_{\mathbf{q}s}^\dagger e^{-i(\mathbf{q} \cdot \mathbf{r}_k - \omega_q t)} + \text{h.c.}) \cdot \underbrace{(\sigma_k^+ e^{it(\omega_a + V \sum_{m \in \mathcal{I}_k} n_m)} + \text{h.c.})}_{\mathcal{X}_k(t)}. \quad (\text{S6})$$

We label all atoms in the neighborhood of atom k with $m \in \mathcal{I}_k$.

Afterwards we introduce the projectors motivated and defined in figure (1) of the main paper. This allows the exponential term in $\mathcal{X}_k(t)$ to be represented in the basis of the neighbouring atoms. For $\mathcal{X}_k(t)$ one obtains:

$$\mathcal{X}_k(t) = \sigma_k^+ e^{it\omega_a} \sum_{\xi=0}^{2d} P_k^\xi e^{it\xi V} + \text{h.c.} \quad (\text{S7})$$

We substitute $H''(t)$ from (S6) into the Markovian quantum master equation (S2). First, we simplify the occurring double commutator expression in (S2). For the bath, we assume the vacuum state, i.e., a temperature $T = 0$. Thus, according to [42], we have for the expectation values of the bath operators:

$$\langle a_{\mathbf{q}} \rangle = \langle a_{\mathbf{q}}^\dagger \rangle = \langle a_{\mathbf{q}} a_{\mathbf{q}'} \rangle = \langle a_{\mathbf{q}}^\dagger a_{\mathbf{q}'}^\dagger \rangle = \langle a_{\mathbf{q}}^\dagger a_{\mathbf{q}'} \rangle = 0 \quad \text{and} \quad \langle a_{\mathbf{q}} a_{\mathbf{q}'}^\dagger \rangle = \delta_{\mathbf{q}, \mathbf{q}'} . \quad (\text{S8})$$

After applying the trace over the degrees of freedom of the bath, the double commutator reads:

$$\begin{aligned} & \text{tr}_E \left\{ \sum_{k, k'} \sum_{\mathbf{q}, \mathbf{q}'} \sum_{s, s'} [H''_{\mathbf{q}k}(t), [H''_{\mathbf{q}'k'}(t - \tau), \rho_{\text{int}} \otimes \rho_E(0)]] \right\} \\ &= \sum_{k, k'} \sum_{\mathbf{q}s} |g_{\mathbf{q}s}|^2 e^{i\mathbf{q} \cdot \mathbf{r}_{kk'}} [\mathcal{X}_k(t), \mathcal{X}_{k'}(t - \tau) \rho_{\text{int}}] e^{-i\omega_q \tau} + \text{h.c.} . \end{aligned} \quad (\text{S9})$$

Note that we now sum up pairwise over all atoms with index k and k' . If we add up all the intermediate results, the Markov master equation looks like this:

$$\dot{\rho}_{\text{int}} = - \sum_{k, k'} \sum_{\mathbf{q}s} |g_{\mathbf{q}s}|^2 e^{i\mathbf{q} \cdot \mathbf{r}_{kk'}} \int_0^\infty d\tau [\mathcal{X}_k(t), \mathcal{X}_{k'}(t - \tau) \rho_{\text{int}}] e^{-i\omega_q \tau} + \text{h.c.} ,$$

where we have already interchanged integration and summation.

Next, we consider the integration of the time difference $d\tau$. To do this, we insert the expression for $\mathcal{X}_k(t)$ from (S7) and multiply the entire expression out. Summand by summand integrals of similar form are to be solved. Using the formula from [42]:

$$\int_0^\infty d\tau e^{-i\tau(\omega_q \pm \omega_a)} = \pi \delta(\omega_q \pm \omega_a) - i\mathcal{P} \left(\frac{1}{\omega_q \pm \omega_a} \right) \quad (\text{S10})$$

and application of the rotating wave approximation for all fast oscillating terms with factors $\mathcal{O}(e^{itV})$ or $\mathcal{O}(e^{2itV})$, the equation can be further simplified.

Now the Markovian master equation is in a known form for several interacting atoms. The summation over the bath modes \mathbf{q} with polarisation s is transformed into an integration analogously to what done in Ref. [24]. After solving this one obtains a Markovian master equation:

$$\dot{\rho}_{\text{int}} = \sum_{\xi=0}^{2d} \left(-i \sum_{k \neq k'} \tilde{V}_{kk'}^\xi \left[\sigma_k^+ P_k^\xi P_{k'}^\xi \sigma_{k'} , \rho_{\text{int}} \right] + \sum_{k, k'} \tilde{\Gamma}_{kk'}^\xi \left[\sigma_{k'} P_{k'}^\xi \rho_{\text{int}} P_k^\xi \sigma_k^+ - \frac{1}{2} \left\{ \sigma_k^+ P_k^\xi P_{k'}^\xi \sigma_{k'} , \rho_{\text{int}} \right\} \right] \right) . \quad (\text{S11})$$

Where

$$\tilde{V}_{kk'}^\xi = -\frac{3\gamma^\xi}{4} \left[\alpha_{kk'} \frac{\cos b_{kk'}}{b_{kk'}} - \beta_{kk'} \left(\frac{\sin b_{kk'}}{b_{kk'}^2} + \frac{\cos b_{kk'}}{b_{kk'}^3} \right) \right] , \quad (\text{S12})$$

$$\tilde{\Gamma}_{kk'}^\xi = \frac{3\gamma^\xi}{2} \left[\alpha_{kk'} \frac{\sin b_{kk'}}{b_{kk'}} + \beta_{kk'} \left(\frac{\cos b_{kk'}}{b_{kk'}^2} - \frac{\sin b_{kk'}}{b_{kk'}^3} \right) \right] , \quad (\text{S13})$$

utilizing $b_{kk'} = \omega_a |\mathbf{r}_{kk'}|/c = 2\pi |\mathbf{r}_{kk'}|/\lambda_a$, $\alpha_{kk'} = 1 - (\mathbf{d} \cdot \mathbf{r}_{kk'})^2$, $\beta_{kk'} = 1 - 3(\mathbf{d} \cdot \mathbf{r}_{kk'})^2$ and $\gamma^\xi = |\mathbf{d}^2|(\omega_a + \xi V)^3/3\pi\epsilon_0 c^3$.

We use now the assumptions of our model where $\omega_a \ll V$ thus $\gamma^\xi \approx \gamma$. Furthermore we use the fact that we are in a regime where the distance $|\mathbf{r}_{kk'}|$ between the Rydberg atoms is large with respect to the wavelength of the atomic transition λ_a . Therefore the off-diagonal elements of $\tilde{V}_{kk'}$ and $\tilde{\Gamma}_{kk'}$ vanish. Moreover $\tilde{\Gamma}_{kk'}^\xi \approx \gamma \forall k = k'$. Using the fact $\sum_\xi P_k^\xi = 1$ to simplify the anti-commutator we obtain:

$$\dot{\rho}_{\text{int}} = \gamma \sum_k \left[\sum_{\xi=0}^{2d} \sigma_k^- P_k^\xi \rho_{\text{int}} P_k^\xi \sigma_k^+ - \frac{1}{2} \{n_k, \rho_{\text{int}}\} \right] . \quad (\text{S14})$$

Measurements and simulations are always carried out in the laboratory frame. For this reason, we transform back into the same laboratory frame. It is valid using the chain rule and with U from (S5):

$$\frac{\partial}{\partial t} \rho = \frac{\partial}{\partial t} (U^\dagger \rho_{\text{int}} U) = -i[H_{\text{atom}}, \rho] + U^\dagger \dot{\rho}_{\text{int}} U . \quad (\text{S15})$$

Let us now consider further the dissipative term. We apply Eq. (S14) and obtain:

$$U^\dagger \dot{\rho}_{\text{int}} U = \gamma \sum_k \left[\sum_{\xi=0}^{2d} \underbrace{U^\dagger \sigma_k^- P_k^\xi \rho_{\text{int}} P_k^\xi \sigma_k^+ U}_{=: \mathcal{J}_1} - \frac{1}{2} \underbrace{U^\dagger \{n_k, \rho_{\text{int}}\} U}_{=: \mathcal{J}_2} \right]. \quad (\text{S16})$$

It can be easily shown by recalculation that:

$$U^\dagger \sigma_k^- P_k^\xi U = e^{i\varphi} \sigma_k^- P_k^\xi \quad (\text{S17})$$

holds, where $\varphi \in \mathbb{R}$. Taking advantage of this identity, we transform the term \mathcal{J}_1 :

$$\mathcal{J}_1 = U^\dagger \sigma_k^- P_k^\xi \rho_{\text{int}} P_k^\xi \sigma_k^+ U \quad (\text{S18})$$

$$= U^\dagger \sigma_k^- P_k^\xi U U^\dagger \rho_{\text{int}} U U^\dagger P_k^\xi \sigma_k^+ U \quad (\text{S19})$$

$$= e^{i\varphi} \sigma_k^- P_k^\xi \rho P_k^\xi \sigma_k^+ e^{-i\varphi} \quad (\text{S20})$$

$$= \sigma_k^- P_k^\xi \rho P_k^\xi \sigma_k^+. \quad (\text{S21})$$

We find that the jump operators do not change due to the transformation into the laboratory frame. For the transformation of \mathcal{J}_2 , it follows analogously:

$$\mathcal{J}_2 = U^\dagger \{n_k, \rho_{\text{int}}\} U = \{n_k, \rho\}. \quad (\text{S22})$$

It follows:

$$\dot{\rho} = -i[H_{\text{atom}}, \rho] + \gamma \sum_k \left[\sum_{\xi=0}^{2d} \sigma_k^- P_k^\xi \rho P_k^\xi \sigma_k^+ - \frac{1}{2} \{n_k, \rho\} \right], \quad (\text{S23})$$

which is the master equation with collective jump operators in the laboratory frame Eq. (5) from the main paper.

II. DECOHERENCE DYNAMICS

We analyse the time evolution of the coherence $X(t)$ defined in Eq. (6) in the main paper. The time evolution can be calculated with the Lindblad operator \mathcal{L} of the system:

$$\frac{\partial}{\partial t} \langle X(t) \rangle = \langle \mathcal{L}^\dagger X(t) \rangle = \underbrace{i[H_{\text{atom}}, X(t)]}_{\text{coherent}} + \underbrace{\mathcal{D}^\dagger[X(t)]}_{\text{dissipative}}. \quad (\text{S24})$$

The coherent part of the evolution is the same for both collective and single-atom dissipation. For the observable $P_k^\xi \sigma_k^-$, this time evolution reads

$$i[H_{\text{atom}}, P_k^\xi \sigma_k^-] = i \frac{V}{2} \sum_{l, m \in \mathcal{I}_l} \left[n_l n_m, P_k^\xi \sigma_k^- \right] + i\omega_a \sum_l \left[n_l, P_k^\xi \sigma_k^- \right], \quad (\text{S25})$$

where we have labelled all atoms in the neighborhood of atom l with $m \in \mathcal{I}_l$. By using the canonical commutator relations for Pauli matrices and the relations

$$\sum_{m \in \mathcal{I}_l} n_m = \sum_{\eta=0}^{2d} \eta P_l^\eta \quad (\text{S26})$$

$$[n_k, P_l^\xi] = 0 \quad \forall k, l \quad (\text{S27})$$

one can easily obtain

$$i[H_{\text{atom}}, X_\xi(t)] = -i(\omega_a + \xi V) X_\xi(t). \quad (\text{S28})$$

The dissipative part yields different results depending on whether the collective or single-atom approach is considered. For the collective approach we evaluate:

$$\mathcal{D}_c^\dagger[P_k^\xi \sigma_k^-] = \gamma \sum_m \left[\sum_{\eta=0}^{2d} P_m^\eta \sigma_m^+ P_k^\xi \sigma_k^- P_m^\eta \sigma_m^- - \frac{1}{2} \{n_m, P_k^\xi \sigma_k^-\} \right] = -\gamma \left(\frac{1}{2} P_k^\xi \sigma_k^- + \sum_{m \in \mathcal{I}_k} n_m P_k^\xi \sigma_k^- \right). \quad (\text{S29})$$

After applying Eq. S26 we find that

$$\mathcal{D}_c^\dagger[X_\xi(t)] = -\gamma \left(\frac{1}{2} + \xi \right) X_\xi(t). \quad (\text{S30})$$

On the other hand, in the single-atom dissipation case, one obtains

$$\mathcal{D}_s^\dagger[P_k^\xi \sigma_k^-] = \gamma \sum_m \left[\sigma_m^+ P_k^\xi \sigma_k^- \sigma_m^- - \frac{1}{2} \{n_m, P_k^\xi \sigma_k^-\} \right] \quad (\text{S31})$$

$$= -\gamma \left(\frac{1}{2} P_k^\xi \sigma_k^- + \xi P_k^\xi \sigma_k^- - \sum_{m \in \mathcal{I}_k} \sigma_m^+ P_k^\xi \sigma_m^- \sigma_k^- \right). \quad (\text{S32})$$

Again, applying Eq. S26 we find that

$$\mathcal{D}_s^\dagger[X_\xi(t)] = -\gamma \left(\frac{1}{2} + \xi \right) X_\xi(t) + \gamma(\xi + 1) X_{\xi+1}(t). \quad (\text{S33})$$

III. MEAN FIELD EQUATIONS

In general, starting from a master equation in Lindblad form with operator \mathcal{L} [42], one can derive a system of equations of motion for an observable A with:

$$\left\langle \frac{\partial}{\partial t} A(t) \right\rangle = \langle A \mathcal{L} \rho(t) \rangle. \quad (\text{S34})$$

In the analysis of our system, the average number of excitations in the system, normalized by the number of particles N , is of interest. We define this quantity as the excitation density $\langle n \rangle$ of the system with:

$$\langle n \rangle = \frac{1}{N} \sum_{k=1}^N n_k. \quad (\text{S35})$$

Based on the two master equations we have obtained, for collective and single-atom dissipation, the equations of motion for $\langle n \rangle$ are now derived. In the calculation with the collective Lindbladian \mathcal{L}_c , an additional factor $4d \langle n \rangle$ appears, which results from the contribution of neighbouring atoms. For N atoms, one obtains a set with $3N$ independent equations.

Now we assume translation-invariance in the system, i.e., $\langle n_k \rangle = \langle n_{k'} \rangle = \langle n \rangle$. This reduces the $3N$ independent equations to just three equations:

$$\begin{aligned} \langle \dot{n} \rangle &= \Omega \langle \sigma_y \rangle - \gamma \langle n \rangle \\ \langle \dot{\sigma}_x \rangle &= -\Delta \langle \sigma_y \rangle - \frac{\gamma}{2} (4d \langle n \rangle + 1) \langle \sigma_x \rangle - 2dV \langle n \rangle \langle \sigma_y \rangle \\ \langle \dot{\sigma}_y \rangle &= -\Delta \langle \sigma_x \rangle - \frac{\gamma}{2} (4d \langle n \rangle + 1) \langle \sigma_y \rangle + 2dV \langle n \rangle \langle \sigma_x \rangle - \Omega (4 \langle n \rangle - 2), \end{aligned} \quad (\text{S36})$$

where approximation $\langle n \sigma_x \rangle = \langle n \rangle \langle \sigma_x \rangle$ has been applied.